Interactive dynamics of two copropagating laser beams in underdense plasmas

Hui-Chun Wu, Zheng-Ming Sheng, and Jie Zhang
Laboratory of Optical Physics, Institute of Physics, Chinese Academy of Science, Beijing 100080, China
(Received 31 March 2004; published 31 August 2004)

The interaction of two copropagating laser beams with crossed polarization in the underdense plasmas has been investigated analytically with the variational approach and numerically. The coupled envelope equations of the two beams include both the relativistic mass correction and the ponderomotive force effect. It is found that the relativistic effect always plays the role of beam attraction, while the ponderomotive force can play both the beam attraction and beam repulsion, depending upon the beam diameters and their transverse separation. In certain conditions, the two beam centers oscillate transversely around a propagation axis. In this case, the ponderomotive effect can lead to a higher oscillation frequency than that accounting for the relativistic effect only. The interaction of two beams decreases the threshold power for self-focusing of the single beam. A strong self-trapping beam can channel a weak one.

DOI: 10.1103/PhysRevE.70.026407 PACS number(s): 52.35.Mw, 42.65.−k, 52.38.Hb

Because of some nonlinear effects, a laser beam with high enough power can modify the material refraction index. The refraction index change ΔN resembles the intensity profile of the beam, forming an optical lens that focuses the beam. This is the well-known self-focusing phenomenon. When the self-focusing exactly balances diffraction, the beam becomes self-trapping with a nearly constant or slightly oscillating beam diameter. It is thus to form an optical spatial soliton [1]. The $(2+1)$D optical spatial solitons are unstable in the Kerr media, which is characterized by $\Delta N=n_2 I$, where I is the local intensity and n_2 is the nonlinear refraction index. The laser beam suffers from catastrophic self-focusing and eventually breaks up. However, it is found that materials with saturable nonlinearities are able to prevent catastrophic collapse [1]. The $(2+1)$D optical spatial solitons in the saturable media, such as photorefractive materials and plasmas, have been investigated theoretically and experimentally. Laser power for forming the optical spatial soliton ranges from only μW in the photorefractive material [2] to TW in the plasmas [3]. Recently, there has been much interest in the interaction between two optical spatial solitons, which are either parallel to each other or crossed at some angles. This kind of interaction exhibits many striking features, such as attraction, fusion [4], repulsion, fission [5], and spiraling [6,7].

In plasmas, the nonlinear effects responsible for self-focusing are relativistic electron mass correction and the plasma density modification due to the laser ponderomotive effect. The effective refraction index in plasma is $N=[1-n/(\gamma n_c)]^{1/2}$, where γ is the relativistic factor of electron motion, and n and n_c are the electron density and the plasma critical density, respectively. The combined effect of the relativistic mass correction and the density modification leads to a self-focusing lens, where $\Delta N \leqslant 1$. The critical laser power for relativistic self-focusing in plasmas is $17(\omega/\omega_p)^2$GW [3], where ω is the light frequency and $\omega_p=(4\pi ne^2/m_e)^{1/2}$ is the electron plasma frequency. Recently, we have investigated the interaction between two copropagating laser beams with the same polarization directions in underdense plasmas, and found that two beams can merge into one beam or split into three beams under different circumstances [8]. Ren *et al.* have observed spiraling of the two beams with crossed polarization directions in particle-in-cell (PIC) simulations [7]. They also have studied this phenomenon analytically, where their coupled beam equations only include the effect of the relativistic mass correction. However, the plasma density modification due to the laser ponderomotive force, which has a significant influence on the self-trapping of a laser beam [3], has been ignored.

In this paper, we study the interaction of copropagating beams with coupled envelope equations including both the relativistic mass correction and the ponderomotive force effect. Using the variational method [7,9], we obtain a set of ordinary differential equations to describe the beam centers and diameters, etc. The result is compared with what is found by directly solving the coupled equations numerically.

The coupled evolution equations for two laser beams with crossed polarization directions in underdense plasmas can be written as [3,10]

$$2i\frac{\partial a_{1,2}}{\partial \tau}+\nabla_\perp^2 a_{1,2}=\frac{n}{\gamma}a_{1,2}, \tag{1}$$

where a_1 and a_2 are the slowly varying vector potentials of the two beams normalized by mc^2/e, respectively, the relativistic factor $\gamma=\sqrt{1+(|a_1|^2+|a_2|^2)/2}$, and the density $n=\max(0,1+\nabla_\perp^2\gamma)$ addressing the ponderomotive expulsion of electron density from the high-intensity regions, which is normalized by the unperturbed plasma density n_0. Here $\tau=\omega_p^2 t/\omega$ and $\nabla_\perp^2=\partial^2/\partial x^2+\partial^2/\partial y^2$ with transverse coordinate x and y normalized by c/ω_p. At the weakly relativistic approximation, $n/\gamma\approx 1-\frac{1}{4}(1-\nabla_\perp^2)(|a_1|^2+|a_2|^2)$. Substituting n/γ into Eq. (1), we obtain the following coupled nonlinear equations:

$$2i\frac{\partial a_1}{\partial \tau}+\nabla_\perp^2 a_1-a_1+\frac{1}{4}a_1(1-\nabla_\perp^2)(|a_1|^2+|a_2|^2)=0,$$

$$2i\frac{\partial a_2}{\partial \tau}+\nabla_\perp^2 a_2-a_2+\frac{1}{4}a_2(1-\nabla_\perp^2)(|a_1|^2+|a_2|^2)=0, \tag{2}$$

where term $a_{1,2}(|a_1|^2+|a_2|^2)$ and term $a_{1,2}\nabla_\perp^2(|a_1|^2+|a_2|^2)$ represent the relativistic mass correction and the ponderomotive force effect, respectively.

Approximate solutions of Eq. (2) can be obtained by using the variation method [7]. First, we need to find a Lagrangian density $\mathcal{L}$, where the Euler-Lagrange equations can reproduce Eq. (2) by minimizing the action $\int_{-\infty}^{\infty}\mathcal{L}d\tau dxdy$. Such a Lagrangian density is

$$\mathcal{L}=\sum_{j=1,2}\left[i\left(a_j\frac{\partial a_j^*}{\partial\tau}-a_j^*\frac{\partial a_j}{\partial\tau}\right)+|a_j|^2-\frac{1}{8}|a_j|^4+\left(1+\frac{1}{4}|a_j|^2\right)\boldsymbol{\nabla}_\perp a_j\cdot\boldsymbol{\nabla}_\perp a_j^*+\frac{1}{8}|a_j|^2(a_j\nabla_\perp^2 a_j^*+a_j^*\nabla_\perp^2 a_j)\right]+\mathcal{L}_{12}, \tag{3}$$

where a_j^* is the complex conjugate and $\mathcal{L}_{12}=-1/4(|a_1|^2|a_2|^2+\boldsymbol{\nabla}_\perp|a_1|^2\cdot\boldsymbol{\nabla}_\perp|a_2|^2)$. We use the following Gaussian trial functions:

$$a_j=a_{0j}\exp(-i\phi_j)\exp\{-i[k_{xj}(x-X_{cj})+k_{yj}(y-Y_{cj})]\}\exp\{[(x-X_{cj})^2+(y-Y_{cj})^2](i/2R_j-1/W_j^2)\}$$

as in Ref. [7], where the amplitude a_{0j}, phase ϕ_j, beam center (X_{cj},Y_{cj}), perpendicular momentum (k_{xj},k_{yj}), radius of curvature R_j, and the spot size W_j are all real and are functions of τ only. Substituting the trial functions into Eq. (3) and integrating the Lagrangian density $\mathcal{L}$ in the xy plane leads to a reduced Lagrangian density,

$$\begin{aligned}L&\equiv\frac{2}{\pi}\int_{-\infty}^{\infty}dx\int_{-\infty}^{\infty}\mathcal{L}dy\\&=\sum_{j=1,2}\left\{a_{0j}^2W_j^2[-2(\phi_{j\tau}-k_{xj}X_{cj\tau}-k_{yj}Y_{cj\tau})+1+k_{xj}^2+k_{yj}^2]+2a_{0j}^2-\frac{1}{4}a_{0j}^4-\frac{1}{16}a_{0j}^4W_j^2+\frac{1}{2}a_{0j}^2W_j^4\frac{(1-R_{j\tau})}{R_j^2}\right\}\\&\quad-\frac{a_{01}^2a_{02}^2W_1^2W_2^2}{W_1^2+W_2^2}\exp\left(\frac{-2d^2}{W_1^2+W_2^2}\right)\left\{\frac{1}{4}+\frac{2}{W_1^2+W_2^2}+\frac{4}{W_1^2+W_2^2}[(\alpha_X-X_{c1})(\alpha_X-X_{c2})+(\alpha_Y-Y_{c1})(\alpha_Y-Y_{c2})]\right\},\end{aligned} \tag{4}$$

where $\alpha_X=(X_{c1}W_2^2+X_{c2}W_1^2)/(W_1^2+W_2^2)$, $\alpha_Y=(Y_{c1}W_2^2+Y_{c2}W_1^2)/(W_1^2+W_2^2)$, and $d=\sqrt{(X_{c1}-X_{c2})^2+(Y_{c1}-Y_{c2})^2}$ is the distance between the centers of the two beams. One can find the evolution equations of the beam parameters by Euler-Lagrange equations for the reduced Lagrangian density L: $\partial L/\partial\beta-(d/d\tau)\partial L/\partial\dot{\beta}+(d^2/d\tau^2)\partial L/\partial\ddot{\beta}=0$, where β is any variational parameter for the laser beams.

Varying ϕ_j leads to the power conservation $d(a_{0j}^2W_j^2)/d\tau=0$. Varying R_j, one obtains $W_j/R_j=dW_j/d\tau$. By varying W_j, the equations for the evolution of each beam spot size are given as

$$\begin{aligned}\frac{d^2W_j}{d\tau^2}+\frac{4}{W_j^3}\left(\frac{P_j}{32}-1\right)+\frac{P_j}{W_j^5}&=\frac{P_1P_2}{2(W_1^2+W_2^2)^2}\frac{W_j}{P_j}\exp\left(\frac{-2d^2}{W_1^2+W_2^2}\right)\left(-1+\frac{2d^2}{W_1^2+W_2^2}\right)+\frac{8P_1P_2}{(W_1^2+W_2^2)^3}\frac{W_j}{P_j}\exp\left(\frac{-2d^2}{W_1^2+W_2^2}\right)\\&\quad\times\left\{\left(-1+\frac{d^2}{W_1^2+W_2^2}\right)[1+2(\alpha_X-X_{c1})(\alpha_X-X_{c2})+2(\alpha_Y-Y_{c1})(\alpha_Y-Y_{c2})]\right.\\&\quad\left.+[(2\alpha_X-X_{c1}-X_{c2})(\alpha_X+X_{c\bar{j}})+(2\alpha_Y-Y_{c1}-Y_{c2})(\alpha_Y+Y_{c\bar{j}})]\right\},\end{aligned} \tag{5}$$

where

$$\bar{j}=\begin{cases}1, j=2\\2, j=1.\end{cases}$$

The left-hand side of Eq. (5) determines the evolution of each beam itself due to the relativistic effect, beam diffraction, and the ponderomotive force. The right-hand side of Eq. (5) shows the effect of the beam interaction through the relativistic effect and the ponderomotive force. From Eq. (5), neglecting the right-hand side, one obtains that the normalized threshold power of relativistic self-focusing for individual beams is reached when $P_j\geqslant P_c\equiv 32$. On the other hand, let us consider the propagation of a weak beam two in the background of another powerful beam one with $P_2\ll P_1$ and $P_2\ll 32$. If the two beams propagate in a coaxis, so that $d=0$, $X_{cj}=Y_{cj}=0$, and $\alpha_X=\alpha_Y=0$, then one finds that beam two can be guided without diffraction through the relativistic effect if the power of the beam one $P_1\geqslant 8(1+W_1^2/W_2^2)^2$, which can be less than 32 provided $W_1<W_2$.

The motion of the beam centroids can be obtained from varying (k_{xj},k_{yj}) and (X_{cj},Y_{cj}). By varying (k_{xj},k_{yj}), it gives $k_{xj}+dX_{cj}/d\tau=0$ and $k_{yj}+dY_{cj}/d\tau=0$. By varying X_{cj}, one obtains

$$P_1\frac{d^2X_{c1}}{d\tau^2}=\frac{-2P_1P_2(X_{c1}-X_{c2})}{(W_1^2+W_2^2)^2}\exp\left(\frac{-2d^2}{W_1^2+W_2^2}\right)\left\{\frac{1}{4}+\frac{2}{W_1^2+W_2^2}+\frac{4}{W_1^2+W_2^2}[(\alpha_X-X_{c1})(\alpha_X-X_{c2})+(\alpha_Y-Y_{c1})(\alpha_Y-Y_{c2})]\right\}$$
$$+\frac{2P_1P_2}{(W_1^2+W_2^2)^3}\exp\left(\frac{-2d^2}{W_1^2+W_2^2}\right)[\alpha_X(W_2^2-W_1^2)+W_1^2X_{c2}-W_2^2X_{c1}],$$

$$P_2\frac{d^2X_{c2}}{d\tau^2}=\frac{2P_1P_2(X_{c1}-X_{c2})}{(W_1^2+W_2^2)^2}\exp\left(\frac{-2d^2}{W_1^2+W_2^2}\right)\left\{\frac{1}{4}+\frac{2}{W_1^2+W_2^2}+\frac{4}{W_1^2+W_2^2}[(\alpha_X-X_{c1})(\alpha_X-X_{c2})+(\alpha_Y-Y_{c1})(\alpha_Y-Y_{c2})]\right\}$$
$$-\frac{2P_1P_2}{(W_1^2+W_2^2)^3}\exp\left(\frac{-2d^2}{W_1^2+W_2^2}\right)[\alpha_X(W_2^2-W_1^2)+W_1^2X_{c2}-W_2^2X_{c1}]. \quad (6)$$

Similar equations hold in the y direction. Equation (6) shows that the beam centroids move like two particles with the mass proportional to their powers. Momentum conservation $P_1\dot{X}_{c1}+P_2\dot{X}_{c2}=$const can be straightly obtained from Eq. (6).

In a simplified case, assuming $P_1=P_2=P$ and $W_1=W_2=W$, the motion equations of the two beams become

$$\frac{d^2\Delta X_c}{d\tau^2}=\frac{-P}{W^4}\Delta X_c\exp\left(\frac{-d^2}{W^2}\right)\left(\frac{3}{4}+\frac{1}{W^2}-\frac{d^2}{2W^2}\right),$$

$$\frac{d^2\Delta Y_c}{d\tau^2}=\frac{-P}{W^4}\Delta Y_c\exp\left(\frac{-d^2}{W^2}\right)\left(\frac{3}{4}+\frac{1}{W^2}-\frac{d^2}{2W^2}\right), \quad (7)$$

where $\Delta X_c=X_{c1}-X_{c2}$ and $\Delta Y_c=Y_{c1}-Y_{c2}$. As compared with what was obtained in Ref. [7], new terms on the right-hand side of Eq. (7) appear because of the introduction of the ponderomotive force effect in Eq. (2). In the factor $(3/4+1/W^2-d^2/2W^2)$, the relativistic effect contributes only $1/4$ and the ponderomotive force contributes $(1/2+1/W^2-d^2/2W^2)$. This suggests that the relativistic effect always contributes to the beam attraction, while the ponderomotive force can play the role of beam attraction only for a transverse separation between beam centers $d<\sqrt{2+W^2}$, beyond which it plays the role of beam repulsion. Physically, the ponderomotive repulsion is caused by the density increase in space between two beams, which leads to a low refractive index there. The beam repulsion can overcome the relativistic beam attraction when $d>\sqrt{2+3W^2/2}$.

Meanwhile, Eq. (7) can describe oscillating motion of two copropagating beams parallel to each other and spiraling motion for two beams with initial perpendicular momenta or at some crossing angles. For the spiraling motion, their transverse separation distance d can be constant. One obtains the spiraling frequency

$$\Omega=\sqrt{\frac{P}{W^4}\exp\left(\frac{-d^2}{W^2}\right)\left(\frac{3}{4}+\frac{1}{W^2}-\frac{d^2}{2W^2}\right)}$$

from Eq. (7). It is apparent that the spiraling solutions exist while $d<\sqrt{2+3W^2/2}$. Beyond this upper limit, two beams will depart from each other. This has been caused by the repulsive effect of the ponderomotive force. Without accounting for the ponderomotive force, it is also found that there is an upper limit on the beam distance based on the stability analysis of the spiraling motion [7], which is $d<\sqrt{2}W$. The physical meaning for the two limits is obviously different. Under the same conditions as in Ref. [7], we find that the two beams rotate 180° after 552 ω_p^{-1}, which is very close to 540 ω_p^{-1} observed in their PIC simulation. It is noted that, without including the ponderomotive effect, their theory predicts a time of 586 ω_p^{-1} for a rotation of 180°. It appears that due to the ponderomotive effect, the interaction force between the two beams becomes stronger, leading to a higher spiraling frequency.

When two beams propagate parallel to each other, we cannot obtain the oscillating frequency as above and we should solve Eq. (6) or Eq. (7) numerically, since the distance d is variable. To account for more general cases, we solve the coupled equations (1)with the alternating-directing implicit (ADI) method [11]. A rectangular simulation box is used in the x-y plane. The input beams are launched parallel to each other along the z direction, and without initial perpendicular momenta. The transverse beam profiles are in Gaussian focus with $a_i=a_{0i}\exp\{-[(x-X_{0i})^2+y^2]/W_{0i}^2\}$. In the whole simulation processes, the energy center $\langle x\rangle_i$ of the two beams is tracked, where $\langle x\rangle_i=I_{\rm tot}^{-1}\int_{-\infty}^{\infty}x|a_i(x,y)|^2dxdy$ and $I_{\rm tot}=\int_{-\infty}^{\infty}|a_i(x,y)|^2dxdy$. The latter represents the total laser energy [6].

Figure 1 illustrates the evolution of the two beams when $a_{01}=a_{02}=0.15$, $W_{01}=W_{02}=20\sqrt{2}$, and $X_{01}=-X_{02}=12$. Even though the corresponding power for the single beam is $P=18$, much less than P_c, the two beams are still trapped while propagating. It suggests that the interaction of two beams decreases the threshold power for self-focusing of the single beam. This result can be deduced straight from Eq. (2), in which the intensity superposition of the two beams is equivalent to increasing the power of the single beam. As Fig. 1 shows, the width of the two beams slowly changes from $20\sqrt{2}$ to 10 in $\tau\in[0,2000]$. The beam amplitude increases to 0.39 in $\tau=2000$. The two beams attract, intersect, and separate, like a damped oscillation with an increasing oscillation frequency. Based on the assumption that both beams always have constant $W=20\sqrt{2}$, from Eq. (6) one obtains that the two Gaussian beams have a nondamping and sinusoidal oscillation, as shown with the dashed line in Fig. 1(c). The

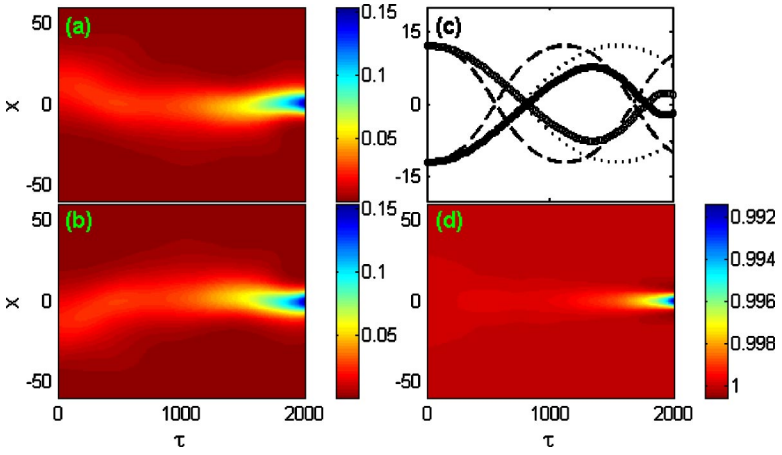

FIG. 1. (Color online) Evolution of two beams with initial parameters: $a_{01}=a_{02}=0.15$, $W_{01}=W_{02}=20\sqrt{2}$, $X_{01}=-X_{02}=12$. (a) $|a_1|^2$; (b) $|a_2|^2$; (c) circles: energy center of the beams, dashed line: theory including both the ponderomotive and relativistic effects, dotted line: theory only including the relativistic effect; and (d) electron density n.

oscillatory period is $T=2244$. The dotted line in Fig. 1(c) shows theory prediction without the ponderomotive effect, and the corresponding oscillatory period is $T=3098$. The theory agrees better with the simulation when including the ponderomotive effect. As mentioned above, the additive ponderomotive effect in Eq. (2) led to stronger interaction and higher oscillatory frequency. Equation (6) also predicts that oscillatory frequency will increase when the beam amplitudes increase and their distance decreases. For $a_{1,2}=0.39$, $W_{1,2}=10$, and $d=4.5$, the oscillatory period $T=207$, which is consistent with the accelerated oscillation in $\tau \in [1750, 2000]$. It is found that the electron density is slightly depressed, as shown in Fig. 1(d).

Figure 2 illustrates another beam evolution when $a_{01}=a_{02}=0.5$, $W_{01}=W_{02}=6.35\sqrt{2}$, and $X_{01}=-X_{02}=5$. The beam width is almost constant in the whole process. The power of one beam is 20.2. It is clear to see that the two beams have an oscillatory motion. The oscillation period of the energy center is about 514 in Fig. 2(c). The electron density also shows a periodic structure, as shown in Fig. 2(d). Our analytical solution from Eq. (6) predicts an oscillation period of $T=349$. This large difference is probably due to the weakly relativistic approximation and the ideal Gaussian beam used in the above variational approach.

The above examples are the cases where the two beams have the same powers. Figure 3 shows the interaction between the two beams with initial parameters: $a_{01}=1$, $a_{02}=0.2$, $W_{01}=W_{02}=3.9\sqrt{2}$, $X_{01}=0$, $X_{02}=-3$. Note that $P_2=1.2$ is much less than $P_1=30.4$. The large power means large mass when one takes an analogy between the laser beams and particles. It is expected that the beam with a small power will twist along the beam with a large power. As shown in Fig. 3, beam one is almost transversely immobile, but beam two oscillates around beam one, with a period of about 200. Meanwhile, beam two remains trapped without significant spreading, even though its power is much lower than the self-focusing threshold. This is also due to the focusing effect of beam one, as also discussed analytically following Eq. (5).

In summary, the interaction of two copropagating laser beams with crossed polarization in the underdense plasma has been investigated analytically and numerically. It is found analytically that the relativistic effect always plays the role of beam attraction, while the ponderomotive force can play the role of both the beam attraction and beam repulsion, depending upon the beam diameters and their center separation. In certain conditions, the two beam centers oscillate transversely around a propagation axis. In this case, the ponderomotive effect can lead to a higher oscillation frequency than that accounting for the relativistic effect only. The interaction between two beams decreases the threshold power for self-focusing of the single beam. A strong self-trapping beam can channel a weak one. Our numerical simulations are consistent with the theoretical analysis in an earlier stage of the beam evolution. In the later stage, the analytical solutions depart from the numerical solutions because of a significant

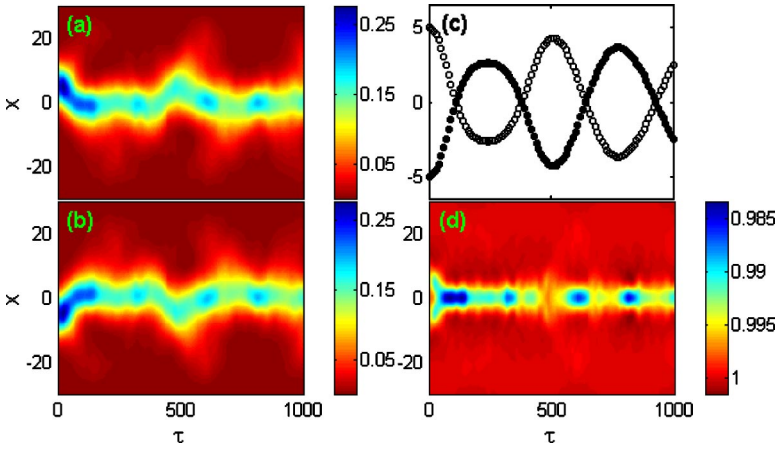

FIG. 2. (Color online) Evolution of two beams with initial parameters: $a_{01}=a_{02}=0.5$, $W_{01}=W_{02}=6.35\sqrt{2}$, $X_{01}=-X_{02}=5$. (a) $|a_1|^2$, (b) $|a_2|^2$, (c) energy center of the beams, and (d) electron density n.

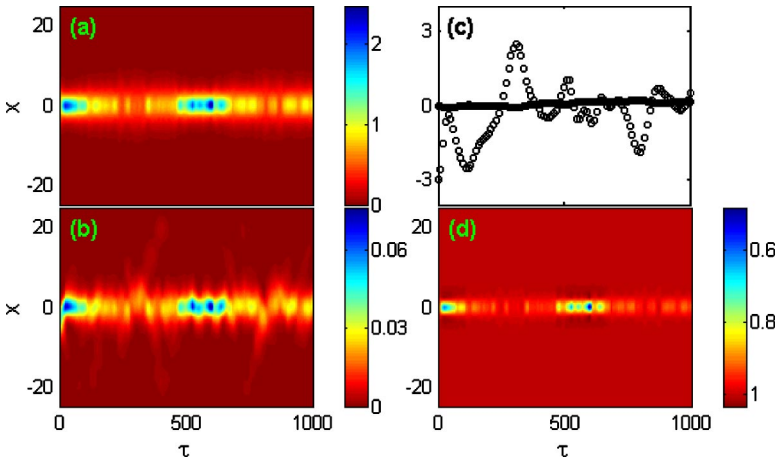

FIG. 3. (Color online) Evolution of two beams with initial parameters: $a_{01}=1$, $a_{02}=0.2$, $W_{01}=W_{02}=3.9\sqrt{2}$, $X_{01}=0$, $X_{02}=-3$. (a) $|a_1|^2$, (b) $|a_2|^2$, (c) energy center of the beams, and (d) electron density n.

change of the beam profile found in the numerical simulations, which is difficult to take into account in the analytical solutions.

It is noted that certain kinetic effects in the plasma, such as electron acceleration and corresponding quasistatic magnetic generation, etc. [12], have been neglected. Usually, these effects are significant in plasmas with moderate densities, but relatively weak in tenuous plasma [13]. Thus the results described above should apply preferably in tenuous plasma such as $n_0/n_c<0.01$. In addition, since we have neglected the longitudinal profiles of laser beams, our results should apply to the case when the durations of the laser beams are much longer than a plasma oscillation period.

This work was supported in part by the National Natural Science Foundation of China (Grants No. 10335020, No. 10105014, and No. 10075075), the National High-Tech ICF Committee in China, and the National Key Basic Research Special Foundation (NKBRSF) under Grant No. G1999075200.

[1] M. Segev and G. Stegeman, Phys. Today **51**(8), 42 (1998); G. I. Stegeman and M. Segev, Science **286**, 1518 (1999).
[2] M. Segev *et al.*, Phys. Rev. Lett. **73**, 3211 (1994).
[3] G. Z. Sun *et al.*, Phys. Fluids **30**, 526 (1987); A. Borisov *et al.*, Phys. Rev. A **45**, 5830 (1992); Z. M. Sheng *et al.*, J. Opt. Soc. Am. B **13**, 584 (1996); Z. M. Sheng and J. Meyer-ter-Vehn, Phys. Rev. E **54**, 1833 (1996).
[4] W. Krolikowski *et al.*, Opt. Lett. **23**, 97 (1998); V. Tikhonenko *et al.*, Phys. Rev. Lett. **76**, 2698 (1996).
[5] L. Torner *et al.*, Opt. Lett. **21**, 462 (1996); W. Krolikowski and S. A. Holmstrom, *ibid.* **22**, 369 (1997); Y. Baek *et al.*, *ibid.* **22**, 1550 (1997).
[6] M. F. Shih *et al.*, Phys. Rev. Lett. **78**, 2551 (1997); A. V. Buryak *et al.*, *ibid.* **82**, 81 (1999); A. Stepken *et al.*, *ibid.* **82**, 540 (1999); M. R. Belic *et al.*, *ibid.* **82**, 544 (1999).
[7] C. Ren *et al.*, Phys. Rev. Lett. **85**, 2124 (2000); C. Ren *et al.*, Phys. Plasmas **9**, 2354 (2002).
[8] Q. L. Dong *et al.*, Phys. Rev. E **66**, 027402 (2002).
[9] D. Anderson, Phys. Rev. A **27**, 3135 (1983); D. Anderson *et al.*, *ibid.* **32**, 2270 (1985).
[10] Z. M. Sheng *et al.*, Phys. Rev. E **64**, 066409 (2001).
[11] W. H. Press *et al.*, *Numerical Recipes in C* (Cambridge University Press, New York, 1992), p. 861.
[12] A. Pukhov and J. Meyer-ter-Vehn, Phys. Rev. Lett. **76**, 3975 (1996).
[13] J. C. Adam *et al.*, Phys. Rev. Lett. **78**, 4765 (1997); G. Malka *et al.*, *ibid.* **79**, 2053 (1997).